Contents lists available at http://qu.edu.iq

Al-Qadisiyah Journal for Engineering Sciences

Journal homepage: https://qjes.qu.edu.iq/

Extended finite element approach to predict and track rupture propagation in abdominal aortic aneurysm

Wisam Al-obaidi [a*], ***Mohammed A. Al-Tayyar*** [b], ***and Parthasarathi Mandal*** [c]

[a]*Department of Mechanical Engineering, Collage of Engineering, University of Al-Qadisiyah, Ad-Diwaniyah, Iraq*
[b]*College of Technical Engineering, University of Al-Kafeel, Iraq: Al-Najaf*
[c]*Department of Mechanical Aerospace and Civil Engineering, The University of Manchester, M13 9PL, UK*

ARTICLE IINFO

Article history:
Received 25 February 2023
Received in revised form 15 April 2023
Accepted 27 July 2023

Keywords:
AAA rupture
XFEM approach
Maximum stress
Life-threatening
Wall strength

ABSTRACT

An abdominal aortic aneurysm (AAA) is a life-threatening cardio-vascular condition. Current surgical intervention is based on the maximum diameter threshold of 5.5 cm. Over the past years, two indicators to predict potential rupture, the Rupture Potential Index (RPI) and Finite Element Analysis Rupture Index (FEARI), had been developed using finite element analysis (FEA), based on the predicted maximum wall stress and statistical or local wall strength. The purpose of this study is to develop a numerical model using the extended finite element method (XFEM) to understand the initiation/growth of potential rupture and predict its location in abdominal aortic aneurysm wall by involving the parameters of failure: the wall stress, wall strength, and strain, as well as, investigating the use of 3D-US AAA models instead of CT models. Failure analyses were conducted on numerical models of AAA derived from 3D-US and CT images for four elected patients to examine the initiation and growth of potential rupture under three different pressures of 120, 140, and 160 mmHg and three different wall strengths of 0.33, 1.34, and 2.36 MPa respectively. The majority of AAAs showed insignificant differences in stress distributions between 3D-US and CT models, except for one patient where the 3D-US model remarkably showed higher stress compared to the CT model. The location of rupture initiation was predicted reliably for both the models of AAA which have been independently verified with visual predictions by cardio-vascular surgeons. However, the predicted length of rupture and the potential penetration (full damage of the wall) varied between the models depending upon the applied pressure and the strength of the wall.

1. Introduction

Aortic wall condition is affected by many factors such as smoking, hypertension, age, gender, etc.[1-3], which may cause irreversible localized inflation (an aneurysm) leading to ruptures [4]. One of these life-threatening aneurysms, especially in the event of rupture [5], is called Abdominal aortic aneurysm (AAA). Abdominal aortic aneurysms can be surgically treated, but it is an expensive procedure associated with a high rate of mortality [6, 7]. Therefore, periodic surveillance of AAA to predict the risk of rupture and its location prior to surgical intervention is vital for saving lives. The current guideline for considering a surgical intervention is when the maximum diameter of AAA reaches 5.5 cm [6, 8]. However, it has been reported that some cases of aneurysms [9, 10] ruptured before reaching the threshold value of 5.5 cm. The rupture process of an aneurysm can be interpreted from a mechanical point of view when the maximum wall stress of AAA induced from the blood flow exceeds the ultimate strength of the AAA wall [11]. To obtain information on the state of stress and strain realistic 3D AAA geometries and mechanical properties of materials such as aortic wall strength and ultimate strain are necessary requirements.

* *Corresponding author.*
E-mail address: wisam.jasim@qu.edu.iq (Wisam Al-obaidi)

https://doi.org/10.30772/qjes.2023.178994

Recently, good-quality patient-specific models of AAAs are being created from medical images CT, MRI, or 3D ultrasound, which can be provided by the hospitals. The mechanical properties of AAA can be obtained from direct physical tests such as uniaxial or biaxial tensile tests, and also from the published literature on previous test data. This information is being increasingly utilized in the process of rupture risk assessment using numerical approaches such as finite element method (FEM) [12-15], computational fluid dynamic (CFD) [16-19] and fluid-structure interaction (FSI) [20-23]. The finite element method is able to successfully predict the rupture site in a number of studies [24, 25]. For instance, a computational model was developed by Vorp et al. [26] to compute the rupture potential index (RPI) as a rupture indicator to determine the possibility of rupture in AAAs. The mathematical formula of RPI combines the predicted maximum wall stress obtained from FEA results with a standalone statistical model used to compute the aneurysmal wall strength [27, 28]. The findings of RPI have identified the risk of rupture better than the ordinary way of maximum diameter criterion [26, 27]. Doyle et al.[29] developed a similar computational model to analyze the risk of rupture called Finite Element Analysis Rupture Index (FEARI). This indicator can be defined as the ratio between the predicted maximum wall stress of a finite element analysis to the local AAA wall strength[30, 31] that corresponds to the predicted location of the maximum stress of AAA wall, where FEARI values range between 0 (low risk of rupture) and 1 (high potential of rupture) [32].
Based on the above, it has been noticed that the following three elements: maximum strength, maximum stress, and maximum strain of the AAA wall should be taken into consideration in the rupture evaluation analysis. However, the previous studies taken one element in consideration which is the maximum stress. In other words, when these three failure factors (stress, strength, and strain) meet at the same place in the diseased wall, this will lead to initiate the rupture in the wall. Interestingly, the Extended Finite Element Method (XFEM), a computational method based on the principles of fracture mechanics being used to evaluate the failure of materials (cracks or rupture[33]), can be employed to achieve numerical modelling of rupture in AAA by engaging the three elements of failure mentioned earlier.

The purpose of this study is to develop a numerical model using XFEM approach to understand the initiation/propagation of potential rupture and predict its location in abdominal aortic aneurysm wall by involving the parameters of failure: the wall stress, wall strength, and strain, as well as, investigating the use of 3D-US AAA models instead of CT models.

2. Methodology

2.1. Image acquisition and construction of AAA geometry

Four patients previously diagnosed with AAA had undergone CT and 3D US scanning test prior to AAA repairing or urgent evaluation at the University Hospital South Manchester were included in this research. National Research Ethics Committee (NREC) (13/NW/0468) has granted ethical approval of using the scanning data. A similar procedure of segmentation using the ImFusion suite [34], see Chapter Four, was followed in this work to create the 3D computational models of AAA derived from 3D-US and CT scans. Subsequently, all the AAA geometries had been exported into Abaqus 2016 [35] for stress and rupture initiation analysis.

2.2. eXtended Finite Element Method in Abaqus

Extended Finite Element Method (XFEM) is a numerical solution technique based on fracture mechanics that combines the ordinary finite element approach and the principle of partition unity to model crack initiation and propagation independently of the mesh size[33]. This approach can handle high discontinuities of displacement in a solution domain by assigning a specific displacement function to enrich and readjust degrees of freedom for a finite element. Equation (1) represents the conventional finite element with the partition of unity method; in other words, the extended finite element method[33]:

$$\boldsymbol{u} = \sum_{i=1}^{N} \boldsymbol{N_i}(\boldsymbol{x}) \left[\boldsymbol{u_i} + \boldsymbol{H}(\boldsymbol{x})\boldsymbol{a_i} + \sum_{\alpha=1}^{4} \boldsymbol{F_\alpha}(\boldsymbol{x})\boldsymbol{b_i^\alpha}\right] \quad (1)$$

Where: $\boldsymbol{u}$ Displacement vector; $\boldsymbol{N_i}$: standard FE function of the node (i),$\boldsymbol{u_i}$: Nodal displacement vectors; $\boldsymbol{H}(\boldsymbol{x})$:Jump function; $\boldsymbol{a_i}$: Nodal enriched degree of freedom vector;$\boldsymbol{F_a}$: Asymptotic crack-tip functions; $\boldsymbol{b_i^\alpha}$: Nodal enriched degree of freedom vector.

The following two steps must meet altogether at one time and one place in order to achieve the initiation and propagation of rupture (crack) within the AAA wall. Firstly, the ratio of the predicted wall stress to the assigned wall strength (0.33, 1.34, and 2.35 MPa) should reach the critical value of a failure factor (f =1) [33] which can be represented by the maximum principal damage criterion as in the following equation:

$$\boldsymbol{f} = \left|\frac{\boldsymbol{AAAstress_{predicted}}}{\boldsymbol{AAAstrength}}\right| \quad (2)$$

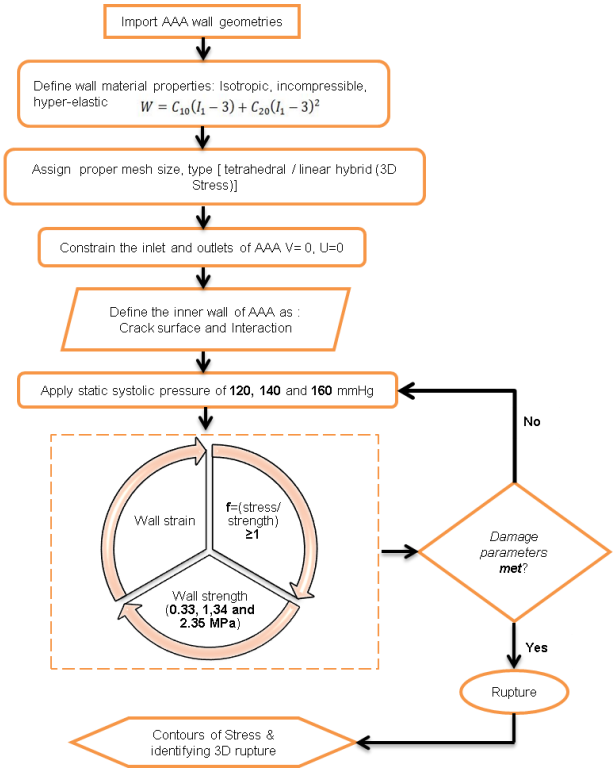

Figure 1: The process of damage criteria and damage initiation in extended finite element simulation used in this work.

Secondly, a damage evolution parameter, maximum strain, corresponds to displacement at failure should be defined and reached. Then, the aneurysmal wall starts to rupture. In the event any one of these two steps or both does not fulfil the damage criteria, the rupture does not occur. Contours of maximum principal stress and virtual 3D rupture are to be requested, see Figure 1.

2.3. Mechanical properties of the blood vessel

Non-linear mechanical properties of blood vessels (AAAs) previously extracted from the uniaxial tensile test [36] that have been widely used in several studies [21, 25, 37-39] were employed. The material library within Abaqus 2016 [35] provides a variety of mathematical models to express the nonlinear behaviour of aneurysmal tissues. In this case, a 2nd order polynomial strain energy mathematical model was utilized:

$$W = C_{10}(I_1 - 3) + C_{20}(I_1 - 3)^2 \quad (3)$$

Where W = strain energy, I_1= the first invariant of the left Cauchy-Green tensor and C_{20}= 1.881 MPa / C_{10}= 0.174 MPa are constants that represent the mechanical wall properties of AAA. The vessel was imposed to behave as isotropic, incompressible, hyperelastic-structure [36, 40]. Further material properties are required by XFEM solution to reach the rupture (crack) initiation and propagation in AAA, such as ultimate strength and strain. Regarding ultimate strength, Raghavan et al.[30]showed that the ultimate regional strength of the AAA wall ranged from 0.336 to 2.35 MPa. Damage criteria of maximum principal stress within Abaqus 2016 [35] was employed to involve the following failure strength of (0.336,1.343 and 2.35 MPa) of the aortic wall in the simulation. In addition, the damage evolution factor is presumed to be the maximum strain of 0.15[30].

2.4. Mesh study and improving the convergence analysis

XFEM approach in Abaqus 2016 [35] is supposed to be independent of the element's size. However, it has been observed that mesh refinement affects the length of the rupture slightly. In this analysis, geometries of AAA walls were meshed in Abaqus 2016 [35] using a hybrid 4-nodes tetrahedron (C3D4H) volumetric element. A systematic mesh independence was performed on AAA1 3D-US, and CT models with low strength, which exposed to a static pressure of 160 mmHg as other pressures of 120 and 140 mmHg will be within the range. The purpose of mesh verification is to investigate the mesh refinement sensitivity against the length of rupture, see Table 1.

Table 1. Mesh independence performed on AAA1.

	CT model		3D-US model	
Mesh No	No. of elements	Rupture length (mm)	No. of elements	Rupture length (mm)
1	163091	9.7	148040	12.5
2	231007	9.8	207375	12.8
3	364585	9.9	342055	13
4	415025	9.9	399279	13.3
5	684552	10	515631	13.3

No significant change has been observed in terms of the rupture length between mesh 4 and 5 in both CT/3D-US models. Therefore, settings of mesh 4 were applied to all geometries. Furthermore, the following settings parameters had to be modified to aid convergence the rupture (crack) initiation analysis successfully:

a) ***Analysis control:*** in most of FEA simulations (continuous domain), default time incrimination parameters $\mathbf{I_0}$ = 4 and $\mathbf{I_R}$ = 8 are utilised to conduct a good performance[41]. However, in rupture (crack) initiation (discontinuous displacement), using default time settings may lead to cutbacks and abortion of the analysis. Thus, the values of I_0 and I_R in this work were changed to 8 and 10, respectively, to increase the number of attempts of each increment and avoiding the cutbacks[42].

b) ***Damage initiation tolerance:*** The initiation of damage sometimes may cause convergence issues[43]. In particular, when the value of the calculated stress at a specific element is higher than the specified magnitude, then the increment size will be reduced by Abaqus 2016 [35]. Subsequently, the specified value of initiation stress cannot be reached in an iterative process, damage tolerance of 0.05 (default) should be defined to initiate the damage in this case. However, to avoid the convergence issues in this study, damage tolerance of 0.001 was prescribed.

c) ***Modifying the number of increments*:** the number of increments I_A was modified to be 50 for the same reason mentioned above.

2.5. Boundary conditions

All aneurysms were constrained upstream and downstream at all directions[44] to simulate the fixed position of the aorta. The presence of intraluminal thrombus and flow forces (shear stresses) were excluded from this simulation because the thrombus can effectively decrease the wall stress[44, 45], and the shear stresses were considered negligible due to no blood flow [46, 47]. In addition, the surrounding organs were imposed, not causing a load at the outer wall of blood vessels, which means the residual stresses in the AAAs wall assumed to be zero[45]. The local variances of the blood vessel thickness cannot be captured by the CT scan; hence, it was presumed to be 2 mm [38, 48-50] and uniformly distributed at all regions of the AAA wall. Hypertension contributes to the formation of AAA and a key factor causing the rupture[51]. Therefore, the AAA geometries were pressurized uniformly to the maximum systolic pressure of 120, 140, and 160 mmHg[12] assuming the patients had hypertension.

3. Validation of XFEM simulation

It is worth to mention here that the use of extended finite element method XFEM in predicting the rupture site in abdominal aortic aneurysms AAAs is a new idea; therefore, there is no numerical data available in the literature to examine the reliability of the current results. On the other hand, due to the complexity of the patient-specific AAAs geometry, seeking for experimental work to rupture an idealized AAA was ideal for examining the validity of the XFEM model. Interestingly, Doyle et al.[52] performed an experimental work to observe the relation between the rupture site and the location of the maximum stress obtained from the FEA simulation for the same AAA silicone model. Therefore, Doyle et al.[52] work was chosen to validate and compare the XFEM results in terms of predicting the rupture site and stress distribution.

3.1. Creating of idealized AAA geometry and Silicon Sluggard 184 material properties

The geometry of the idealized AAA replica was widely used in previous studies [53-56], see figure 2. The experimental rig was replicated numerically using the same boundary conditions and material properties. The mechanical properties of Sluggard 184 silicone were extracted mechanically from tensile test data. It was found that the 3rd Ogden strain energy function within Abaqus 2016 [35] material library captures and fits quite well the hyper-elastic behavior of this material. Table 2 shows the material coefficients used to characterize the 3rd Ogden strain energy function, see equation (1), of the Sluggard 184.

$$W(\lambda_1,\lambda_2,\lambda_3)=\sum_{i=1}^{N}\frac{2\mu_i}{\alpha_i^2}\left(\lambda_1^{\alpha_i}+\lambda_2^{\alpha_i}+\lambda_3^{\alpha_i}-3\right) \quad (4)$$

Table 2: Material coefficients of 3rd Ogden strain energy for Sylgard 184.

	μ	α
1	-304.235	1.2667
2	148.232	1.5962
3	157.156	0.9075

3.2. Boundary conditions and Mesh generation

Two values of static pressure were used in the current numerical simulation. The first pressure was 120 mmHg, representing the average systolic pressure in the cardiac cycle, subject to the internal wall of the idealized AAA with a uniform thickness of 2 mm. The purpose of applying this load was to compare the stress profile between Doyle et al.[52] and the XFEM model along a path starts from the beginning of the AAA sac to a point above the bifurcation. The second load 364.5 mmHg was applied until the AAA reaches the threshold of rupture initiation in order to compare the location of rupture initiation and stress distribution in the idealized AAA between the experimental, FEA, and XFEM results. The numerical model was constraint from moving and rotating at proximal and iliac part representing the experimental rig. Idealized AAA was meshed in Abaqus 2016 [35] using linear and hybrid-tetrahedral of type 3D stress-element (C3D4H). Later, mesh independence study was implemented as reported in section *Mesh study and improving the convergence analysis;* by increasing the number of cells and investigate whether it influences the length of rupture. The number of elements that found to be satisfactory the accuracy of numerical results were 362705 elements.

3.3. Predicted stress distribution and rupture locations

Figure 2 shows a comparison of the predicted stress distributions and rupture initiation location between the XFEM approach and the Experimental/ FEA simulation of Doyle et al.[52]. The red spot at the very left hand of Figure 2 refers to the initiation of rupture observed experimentally (proximal inflection) which is in correspondence with the predicted rupture site (proximal inflection) by the XFEM model (very right hand of Figure 2) at the same load of 364.5 mmHg. In regards to stress distribution, the overall tendency was consistent between the FEA and XFEM results with an insignificant difference due to using two different numerical approaches. These comparisons showed that the XFEM results in good agreement with experimental results[52] and previous numerical studies[57], as well as showed the ability of the XFEM model in predicting the rupture site numerically.

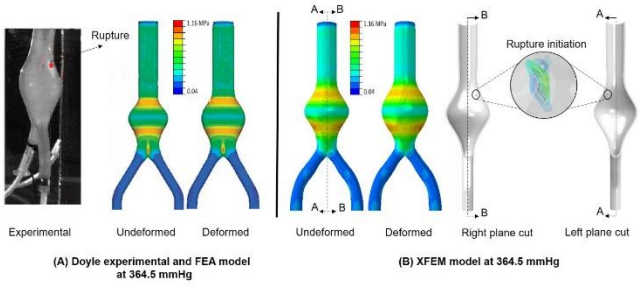

Figure 2. Comparison of the present rupture locations and stress distribution with the experimental work of Doyle et al.[52].

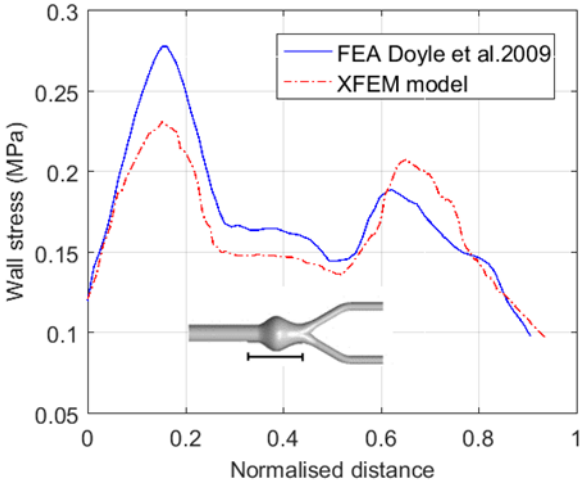

Figure 3. Comparison of wall stress profiles between FEA Doyle et al. and XFEM model.

3.4. Stress trends comparison (FEA vs. XFEM) results

The FEA results of Doyle et al.[52] investigated the effect of wall thickness on the stress trends at 120 mmHg. For the purpose of validation of this work, stress profile from the FEA solution of Doyle et al. [52] for idealised AAA with 2 mm thickness was nominated for comparison with stress profile of the same geometry of 2 mm thickness obtained in XFEM solution. shows a comparison of the AAA wall stress trends between FEA [52] and the XFEM work. It can be seen that the wall stress profiles were fairly comparable, in which the inflection areas (proximal and distal) observed to have high stresses (first peak/ second peak). However, the maximum diameter region was noticed to have lower stress (between the peaks). Rupture risk indicators, RPI and FEARI, mentioned in the introductory part, used the finite element method to predict the site of rupture, which did not involve the strength and strain in the rupture analysis. In this study, three failure parameters (stress, strength, and strain) were

taken into consideration by developing a numerical model of AAA in the extended finite element approach. Comparison of wall stress distribution and rupture initiation/propagation between 3D-US and CT models were obtained to examine the eligibility of using 3D-US AAA models in the rupture analysis.

3.5. AAA wall stress

Comparisons of wall stress distribution in all patients are presented in colour-coded contours in which areas of maximum and minimum stresses are symbolised by red and blue colours respectively. Figure 4, **Error! Reference source not found.**, Figure 6, and Figure 7 show different orientations of AAAs: front, left side, right side, and back in order to facilitate the comparison process.

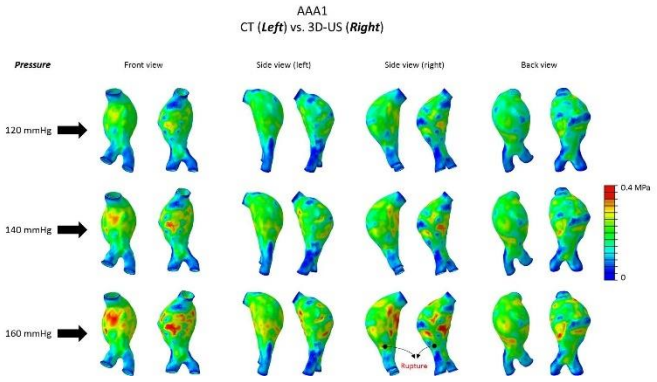

Figure 4. Shows predicted wall stress distribution in AAA1 obtained by XFEM.

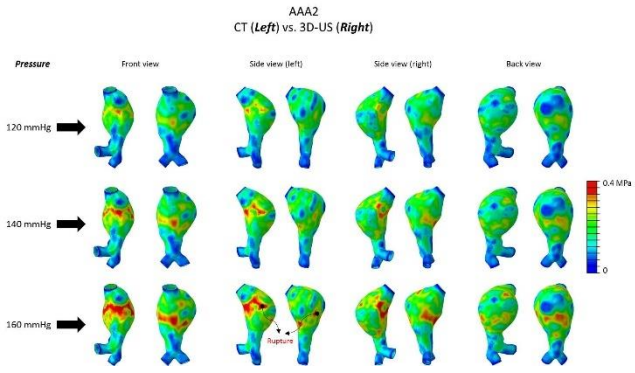

Figure 5. Shows predicted wall stress distribution in AAA2 obtained by XFEM.

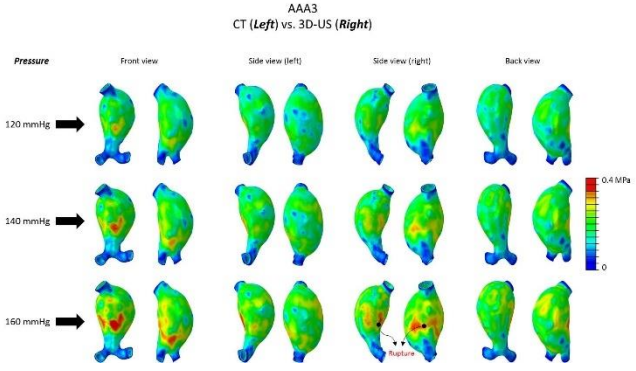

Figure 6. Shows predicted wall stress distribution in AAA3 obtained by XFEM.

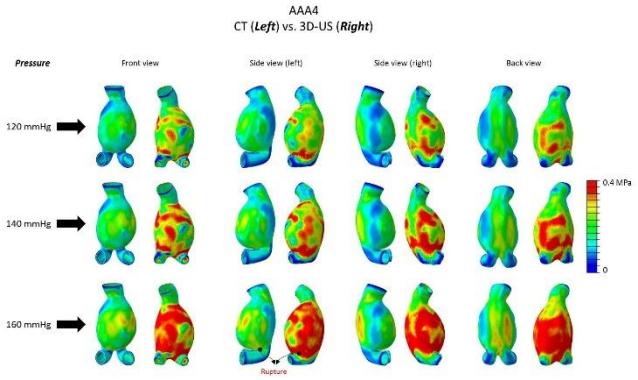

Figure 7. Shows predicted wall stress distribution in AAA4 obtained by XFEM

Values of AAA wall stress ranged from the lowest 0 MPa dark blue to the highest 0.4 MPa dark red in AAA1, AAA2, AAA3, and AAA4 sequentially. In general, it can be observed noticeable differences in the stress distribution between CT and 3D-US models of AAA, to be more specific in the high-stress areas. Low-stress regions of zero MPa in CT and 3D-US AAA models can be simply observed in the bifurcation areas showing no significant influence by increasing the pressure. However, regions of high stress 0.4 MPa in all patients are observed to grow with the increase of the applied pressure significantly. It is also noticed that the location of maximum wall stress remains unaffected by the increase of the load magnitude. AAA4/3D-US in Figure 7 attracts the attention because it shows high sensitivity to pressure magnitude by producing high wall stress of 0.4 MPa, where the red colour almost covers all the aneurysm. In contrast, it is apparent that the stress distribution in CT models increases in a consistent way. The red patches are seen in many places in all patients CT and 3D-US AAA models, but which one of these spots is more likely to rupture? The functionality of using XFEM approach comes to reduce the potential sites of rupture by picking the weakest red spots in the AAA wall where the failure parameters meet together and representing the failure as a 3D crack in the aneurysmal wall.

3.6 Initiation and propagation of rupture

The initiation and propagation of rupture were successfully examined for three different values of pressure and strength by employing the XFEM approach in CT and 3D-US AAA models. A measurement analysis was conducted to measure rupture length in each model of AAAs, based on the increasing of luminal static pressure and wall strength.

Most interestingly, the initiation of rupture is not observed for the average 1.35 MPa and the maximum 2.35 MPa wall strength, even for the 160 mmHg pressure. In contrast, the rupture is observed that begins initiating almost in all aneurysms (CT and 3D-US) when the AAA wall assigned to a low wall strength of 0.33 MPa, then propagates with intensifying of pressure. illustrates a comparison of rupture length between CT and 3D-US models of AAAs at different pressures and AAA low wall strength. Evidently, in , 3D-US AAA models show high tendencies to rupture than the CT models. For instance, the rupture in CT models of AAA1 and AAA3 did not initiate when it pressurised at 120 mmHg, unlike 3D-US models that start rupture.

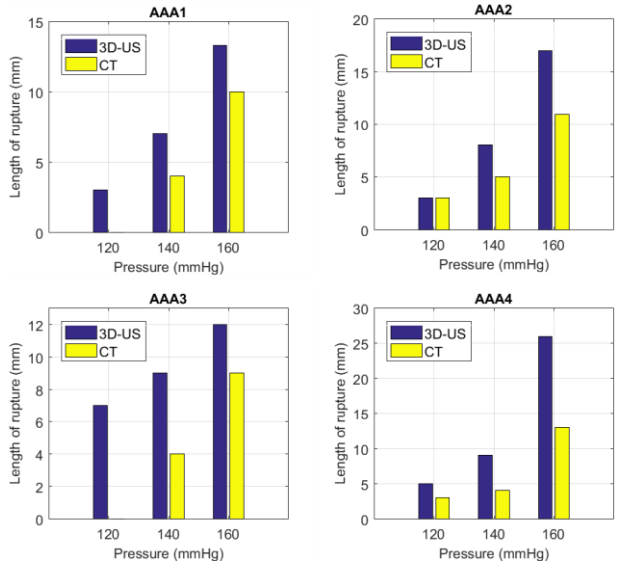

Figure 8. Comparison of rupture length in all AAAs (CT vs. 3D-US) at three different pressures (120, 140, and 160 mmHg) for the lowest wall strength of (0.33 MPa)

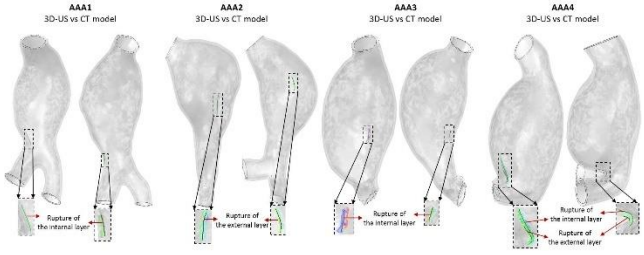

Figure 9. Predicted rupture initiation and location in AAAs wall at160 mmHg and 0.33 MPa wall strength.

Furthermore, the rupture is observed to propagate with the increase of the pressure and, of course, the source of models, where the 3D-US models of AAAs showed high propagations in rupture than the CT models for the same pressure loads. Furthermore, in , the rupture length of AAA4 /3D-US at 160 mmHg is 26 mm, while the CT model is 13 mm.

Strengthening the AAA wall by assigning mean and high wall strengths of 1.34 and 2.35 MPa respectively reveal that the rupture did not occur in both CT and 3D-US models despite the increase of pressure magnitude. The length of rupture is not showing whether a full (rupture) penetration occurs in the AAA wall or not. Therefore, failure (rupture) in the AAA wall can be virtually demonstrated by presenting 3D contours of rupture to show the threatening of bleeding in the AAAs wall. Figure 9 shows the rupture in the CT and 3D-US AAA models for 160 mmHg and low wall strength in all patients. In terms of rupture locations, it is observed to be fairly identical in CT and 3D-US models. For instance, in Figure 9, the rupture tends to happen in the right and left lateral very close to the bifurcation area in AAA1 and AAA4, respectively. However, AAA2 and AAA3, rupture occurs in the left and right lateral far of the bifurcation regions. In terms of full rupture in AAA wall, AAA1 and AAA3 show that the rupture occurs in the internal layer of the AAA wall, whereas the rupture in AAA2 happens in the external layer see Figure 9; which did not lead to full failure in the AAA wall. However, both CT and 3D-US models of AAA4 show full damage in the external and internal layer of the AAA wall, which means full penetration (blood leakage) happens in this patient, see Figure 9. In other words, this patient AAA4 has a high likelihood of rupture and death than other patients because of blood leakage.

4. Discussion

Prior researches about rupture risk assessment in abdominal aortic aneurysms have well documented the efficiency of employing finite element analysis in predicting the location of rupture [12, 15, 25, 37, 58-61] by identifying the location of maximum stress in the AAA wall and reducing the life-threating of unpredictable rupture. Applying non-patient-specific simplified boundary conditions such as linear (isotropic) wall material properties and uniform static pressure were good enough to successfully implementing wall stress analysis [46, 57, 62, 63]. However; this study needed to involve patient-specific AAA models from two different sources and non-linear material properties to obtain more precise results [30, 36].

The current results of wall stress distribution presented in Figure 4, **Error! Reference source not found.**, Figure 6 and Figure 7) showed that the increase of internal pressure on the AAA wall led to a significant increase in the area of maximum wall stress as well as the magnitude, whatever it would be the wall strength. Stress distribution varied throughout the patients owing to many factors such as geometrical differences like tortuosity, the inflection of the AAA surface, irregular shapes [59, 64], and asymmetric [57, 59, 64]. Moreover, using different sources of images (CT and 3D-US) and the segmentation process play an important role in the stress distribution as well. It was observed that the distribution of wall stress highly influenced by the pressure value (hypertension hypothesis)[65], numerical solution, and model source, where 3D-US models showed overestimation in the wall stress distribution as reported in FEA work by Kok et al. [12]. AAA4/3D-US in Figure 7 undoubtedly overestimated wall stress (red area) compared to the CT model of the same patient. However, it did not have multi- rupture despite the wall stress 0.4 MPa overcame the wall strength 0.33 MPa in many locations. This proves that the rupture site needed the three elements of rupture to meet together in one place in order to damage the aneurysmal wall.

It was observed that the strength of the AAA wall did not affect the stress distribution; however, it affected the rupture initiation and propagation in both CT and 3D-US models of AAAs, for instance: The weak AAA wall that had low wall strength of 0.33 MPa was shown high trendies to rupture than other values of strength 1.33 MPa and 2.35 MPa. More interestingly, locations of maximum wall stress did not change with increasing pressure in both CT and 3D-US models. In addition, no relationship was found between maximum wall stress location and the maximum diameter of the aneurysms [37, 60, 66].

XFEM approach used in this analysis provides detailed information regards the predicted stress distribution, rupture length, and shape, unlike the FEA method that provides only stress contours. It was observed that the AAA models regardless the source of imaging did not show any chances of rupture when the wall assigned average and high strength values, because these models of AAAs despite exposing to relatively high pressure 140 and 160 mmHg, it was not sufficient to generate high stress in the AAA wall that overcomes the average and high strength values of 1.35 and 2.35 MPa. Bar charts in showed a comparison of rupture length that propagates with the increase of the internal pressure when the AAA wall has a low strength

of 0.33 MPa. 3D-US models of AAAs firstly started rupture of a length ranged between 3 mm to 7 mm at low 120 mmHg, which then started propagating with the increase of the rupture to reach a range between 12 mm to 26 mm at 160 mmHg. On the other hand, CT models of AAAs showed fewer chances of rupture despite the exposure to the same boundary conditions. For instance, AAA1 and AAA3 did not rupture at 120 mmHg, whereas AAA2 and AAA4 tend to have rupture of length varied from 3 mm to 4 mm at the same pressure. Then, CT models of AAAs that ruptured and those who did not; started initiating and growing the rupture when the internal pressure increased. It is evident from the bar charts that 3D-US AAA models predicted the rupture earlier than the CT models, as well as the rupture site was identical in both.

Although the comparison of rupture propagation in was helpful in terms of providing the relation between pressure and length of rupture in both CT and 3D-US models, the rupture shape and blood leakage is still vague. 3D representation contours of rupture obtained from the XFEM approach in Figure 9 were vital to understanding whether the rupture led to full penetration in the AAA wall or not. The failure in the AAA wall was evident to happen in the internal wall, firstly where the stress intensity is maximum in the AAA wall, as observed in AAA1 and AAA3 in Figure 9. However, the rupture occurred at the external layer of the wall in AAA2. The 3D-US/CT AAA4 predicted failure in both layers of the wall, which means blood leakage, and would have required urgent surgical intervention. The rupture contours can be used to give a good indication of whether the patients need urgent surgery or not. As there is no thrombus formation in AAA3, the predictions of stress and rupture initiation are likely to be more accurate. In other words, the potential of rupture risk in AAA3 may be very close to reality. Figure 9 also shows that the AAA walls fail in the longitudinal directions rather than the circumferential, which is in good agreement with the literature [31]. The XFEM model can be developed for patients regularly to examine the failure/penetration in the AAA wall by comparing the crack length, stress, and penetration to decide which AAA has more potential rupture.

This work has some limitations, such as: ignoring the thrombus in this work was based on findings of Venkatasubramanian et al.[25] that successfully predicted the rupture site without including the thrombus in his work. Furthermore, other studies [45, 67, 68] have found that the thrombus acts as a mechanical cushion and working on reducing the wall stress. Supposing the aneurysmal walls have one value of strength is the second limit of this study, which, in fact, the wall strength is varying locally in the whole wall[30].

5. Conclusion

XFEM, being based on the principles of fracture mechanics, is shown to be suitable for the assessment of rupture potential in the abdominal aortic aneurysm. The good agreement of rupture predictions between the XFEM method and the experimental work in the abdominal aortic aneurysm was found to be applicable for biological materials. The findings of this method provide detailed information about the rupture, such as stress distribution on the aneurysmal wall, length of rupture, site of rupture, and potential of blood leakage, unlike the conventional FEA method that just predicts the rupture site. In addition, the XFEM approach picks only the weak red patches among others that overcome the maximum wall strength, stress, and strain, which reduces the chances of potential rupture in other sites despite having maximum wall stress. In terms of using 3D-US images instead of CT in rupture analysis, it is found that the 3D-US models of AAA show good similarity in predicting the rupture site and predicting the leakage of blood. However, US image-based models show a higher risk of rupture than CT based models. In other words, XFEM findings show that 3D-US is eligible for periodic rupture analysis during the monitoring process of AAA patients due to the availability, no radiation, and affordability of the 3D-US. Accordingly, the approach used here plays as a diagnostic tool for surgeons that may help them to determine if the AAAs require for surgical interventions. The limitations of the current work are as follows: the intraluminal thrombus should be included in the simulation and a more group of patients are needed to increase the prediction reliability.

Authors' contribution

All authors contributed equally to the preparation of this article.

Declaration of competing interest

The authors declare no conflicts of interest.

Funding source

This study didn't receive any specific funds.

Acknowledgements

The authors gratefully acknowledge the financial support by higher committee of education development in Iraq (HCED), and the University of Manchester, MACE school for their support to conduct this work.

REFERENCES

[1] Cheng, C.P., R.J. Herfkens, and C.A. Taylor, *Abdominal aortic hemodynamic conditions in healthy subjects aged 50–70 at rest and during lower limb exercise: in vivo quantification using MRI.* Atherosclerosis, 2003. **168**(2): p. 323-331. http://dx.doi.org/10.1016/s0021-9150(03)00099-6

[2] Larsson, E., et al., *Analysis of aortic wall stress and rupture risk in patients with abdominal aortic aneurysm with a gender perspective.* J Vasc Surg, 2011. **54**(2): p. 295-299 https://doi.org/10.1016/j.jvs.2010.12.053

[3] Samarth, S.R., et al., *Biological, Geometric and Biomechanical Factors Influencing Abdominal Aortic Aneurysm Rupture Risk: A Comprehensive Review*. Recent Patents on Medical Imaging (Discontinued), 2013. **3**(1): p. 44-59. https://doi.org/10.2174/1877613211303010006

[4] Sonesson, B., T. Sandgren, and T. La¨ nne, *Abdominal Aortic Aneurysm Wall Mechanics and their Relation to Risk of Rupture.* Eur J Vasc Endovasc Surg, 1999. **18**: p. 487-493. https://doi.org/10.1053/ejvs.1999.0872.

[5] Piechota-Polanczyk, A., et al., *The Abdominal Aortic Aneurysm and Intraluminal Thrombus: Current Concepts of Development and Treatment.* Frontiers in Cardiovascular Medicine, 2015. https://doi.org/10.3389/fcvm.2015.00019

[6] Moll, F.L., et al., *Management of abdominal aortic aneurysms clinical practice guidelines of the European society for vascular surgery.* Eur J Vasc Endovasc Surg, 2011. 41 Suppl 1: p. S1-S58. https://doi.org/10.1016/s1078-5884(10)00618-0

[7] Imray, C., *Managing an abdominal aortic aneurysm. Practical cardiovascular risk management.* 2006. **4**(2): p. 9-11.

[8] Brown, P.M., D.T. Zelt, and B. Sobolev, *The risk of rupture in untreated aneurysms: the impact of size, gender, and expansion rate*. J Vasc Surg, 2003. **37**(2): p. 280-284. https://doi.org/10.1067/mva.2003.119

[9] Collin, J., *UK small aneurysms trial.* The Lancet, 1999. **353**(9150): p. 407-408. https://doi.org/10.1016/s0140-6736(05)74979-5.

[10] Nicholls, S.C., et al., *Rupture in small abdominal aortic aneurysms.* J Vasc Surg, 1998. **28**(5): p. 884-888.

https://doi.org/10.1016/s0741-5214(98)70065-5.

[11] Thubrikar, M.J., J. Al-Soudi, and F. Robicsek, *Wall stress studies of abdominal aortic aneurysm in a clinical model.* Ann Vasc Surg, 2001. **15**(3): p. 355-366. https://doi.org/10.1007/s100160010080.

[12] Kok, A.M., et al., *Feasibility of wall stress analysis of abdominal aortic aneurysms using three-dimensional ultrasound.* J Vasc Surg, 2015. **61**(5): p. 1175-1184. https://doi.org/10.1016/j.jvs.2014.12.043.

[13] Erhart, P., et al., *Finite Element Analysis in Asymptomatic, Symptomatic, and Ruptured Abdominal Aortic Aneurysms: In Search of New Rupture Risk Predictors*. European Journal of Vascular and Endovascular Surgery, 2015. **49**(3): p. 239-245. https://doi.org/10.1016/j.ejvs.2014.11.010.

[14] Taylor, C.A., T.J.R. Hughes, and C.K. Zarins, *Finite Element Modeling of Three-Dimensional Pulsatile Flow in the Abdominal Aorta: Relevance to Atherosclerosis.* Annals of Biomedical Engineering, 1998. **26**(6): p. 975-987. https://doi.org/10.1114/1.140.

[15] Raghavan, M.L., et al., *Wall stress distribution on three-dimensionally reconstructed models of human abdominal aortic aneurysm.* J Vasc Surg, 2000. **31**(4): p. 760-769. https://doi.org/10.1067/mva.2000.103971.

[16] Li, Z. and C. Kleinstreuer, *Effects of blood flow and vessel geometry on wall stress and rupture risk of abdominal aortic aneurysms.* Journal of Medical Engineering & Technology, 2006. **30**(5): p. 283-297. https://doi.org/10.1080/03091900500217406.

[17] Younis, H.F., et al., *Hemodynamics and wall mechanics in human carotid bifurcation and its consequences for atherogenesis: investigation of inter-individual variation*. Biomech Model Mechanobiol, 2004. **3**(1): p. 17-32. https://doi.org/10.1007/s10237-004-0046-7.

[18] Finol, E.A. and C.H. Amon, *Flow-induced wall shear stress in abdominal aortic aneurysms: Part I--steady flow hemodynamics*. Comput Methods Biomech Biomed Engin, 2002. **5**(4): p. 309-318. https://doi.org/10.1080/1025584021000009742

[19] Owen, B., et al., *Computational hemodynamics of abdominal aortic aneurysms: Three-dimensional ultrasound versus computed tomography*. Proc Inst Mech Eng H, 2016. **230**(3): p. 201-210. https://doi.org/10.1177/0954411915626742.

[20] Leung, J.H., et al., *Fluid structure interaction of patient specific abdominal aortic aneurysms: a comparison with solid stress models.* Biomed Eng Online, 2006. **5**: p. 33-33. https://doi.org/10.1186/1475-925x-5-33.

[21] Scotti, C.M., et al., *Fluid-structure interaction in abdominal aortic aneurysms: effects of asymmetry and wall thickness*. Biomed Eng Online, 2005. **4**: p. 64-64. https://doi.org/10.1186/1475-925x-4-64.

[22] Hoskins, P.R., et al., *Fluid–structure interaction in axially symmetric models of abdominal aortic aneurysms.* Proceedings of the Institution of Mechanical Engineers, Part H: Journal of Engineering in Medicine, 2009. **223**(2): p. 195-209. https://doi.org/10.1243/09544119jeim443.

[23] Gao, F., O. Ohta, and T. Matsuzawa, *Fluid-structure interaction in layered aortic arch aneurysm model: assessing the combined influence of arch aneurysm and wall stiffness*. Australasian Physics & Engineering Sciences in Medicine, 2008. **31**(1): p. 32. https://doi.org/10.1007/bf03178451.

[24] Erhart, P., et al., *Prediction of Rupture Sites in Abdominal Aortic Aneurysms After Finite Element Analysis.* Journal of Endovascular Therapy, 2015. **23**(1): p. 115-120. https://doi.org/10.1177/1526602815612196.

[25] Venkatasubramaniam, A.K., et al., *A comparative study of aortic wall stress using finite element analysis for ruptured and non-ruptured abdominal aortic aneurysms*. Eur J Vasc Endovasc Surg, 2004. **28**(2): p. 168-176. https://doi.org/10.1016/s1078-5884(04)00178-9.

[26] Vande Geest, J.P., et al., *A biomechanics-based rupture potential index for abdominal aortic aneurysm risk assessment.* Ann N Y Acad Sci, 2006. **1085**: p. 11-21. https://doi.org/10.1196/annals.1383.046.

[27] Maier, A., et al., *A comparison of diameter, wall stress, and rupture potential index for abdominal aortic aneurysm rupture risk prediction.* Ann Biomed Eng, 2010. **38**(10): p. 3124-3134. https://doi.org/10.1007/s10439-010-0067-6.

[28] Vande Geest, J.P., et al., *Towards A Noninvasive Method for Determination of Patient-Specific Wall Strength Distribution in Abdominal Aortic Aneurysms*. Annals of Biomedical Engineering, 2006. **34**(7): p. 1098-1106. https://doi.org/10.1007/s10439-006-9132-6.

[29] Doyle, B.J., et al. *A Finite Element Analysis Rupture Index (FEARI) Assessment of Electively Repaired and Symptomatic/Ruptured Abdominal Aortic Aneurysms*. in *6th World Congress of Biomechanics (WCB 2010). August 1-6, 2010 Singapore*. 2010. Berlin, Heidelberg: Springer Berlin Heidelberg. https://doi.org/10.1007/978-3-642-14515-5_225.

[30] Raghavan, M.L., et al., *Regional distribution of wall thickness and failure properties of human abdominal aortic aneurysm.* J Biomech, 2006. **39**(16): p. 3010-3016. https://doi.org/10.1016/j.jbiomech.2005.10.021.

[31] Thubrikar, M.J., et al., *Mechanical properties of abdominal aortic aneurysm wall*. Journal of Medical Engineering & Technology, 2001. **25**(4): p. 133-142. https://doi.org/10.1080/03091900110057806.

[32] Mcgloughlin, T.M., et al., *A Finite Element Analysis Rupture Index (FEARI) as an Additional Tool for Abdominal Aortic Aneurysm Rupture Prediction.* Vascular Disease Prevention, 2009. **9**: p. 114-121. https://doi.org/10.2174/1567270000906010114.

[33] Du, Z.-Z. *eXtended Finite Element Method (XFEM) in Abaqus*. 2009 [cited 2016 10th of March]; Available from: http://www.simulia.com/download/rum11/UK/Advanced-XFEM-Analysis.pdf

[34] *ImFusion suite*. 2015, ImFusion GmbH: München, Germany.

[35] *ABAQUS*. 2016, Simulia, Dassault Systèmes: UK.

[36] Raghavan, M.L. and D.A. Vorp, *Toward a biomechanical tool to evaluate rupture potential of abdominal aortic aneurysm: identification of a finite strain constitutive model and evaluation of its applicability*. Journal of biomechanics, 2000. **33**(4): p. 475-482. https://doi.org/10.1016/s0021-9290(99)00201-8.

[37] Fillinger, M.F., et al., *Prediction of rupture risk in abdominal aortic aneurysm during observation: wall stress versus diameter*. J Vasc Surg, 2003. **37**(4): p. 724-732. https://doi.org/10.1067/mva.2003.213.

[38] Papaharilaou, Y., et al., *A decoupled fluid structure approach for estimating wall stress in abdominal aortic aneurysms.* Journal of Biomechanics, 2007. **40**(2): p. 367-377. https://doi.org/10.1016/j.jbiomech.2005.12.013.

[39] Di Martino, E.S., et al., *Fluid–structure interaction within realistic three-dimensional models of the aneurysmatic aorta as a guidance to assess the risk of rupture of the aneurysm.* Medical Engineering & Physics, 2001. **23**(9): p. 647-655. https://doi.org/10.1016/s1350-4533(01)00093-5.

[40] Kobielarz, M. and L. Jankowski, *Experimental characterization of the mechanical properties of the abdominal aortic aneurysm wall under uniaxial tension*. Vol. 51. 2013. 949-958.

[41] Dassault Systèmes, S.A.C.A.E. *Analysis user's manual volume number ii, analysis procedures, solution, and control*. 2016.

[42] Natarajan, S., D. RoyMahapatra, and S.P.A. Bordas, *A simple integration technique for strong and weak discontinuities in GFEM/XFEM*. Int. J. Numer. Meth. Engng, 2009. https://doi.org/10.1002/nme.2798.

[43] Singh, K., K. Keswani, and M. Vaggar, *Crack growth simulation of stiffened fuselage panels using XFEM techniques*. Vol. 21. 2014. 418-428.

[44] Georgakarakos, E., et al., *The influence of intraluminal thrombus on abdominal aortic aneurysm wall stress*. International Union of Angiology, 2009. **28**(4): p. 325-333.

[45] Wang, D.H., et al., *Effect of intraluminal thrombus on wall stress in patient-specific models of abdominal aortic aneurysm.* J Vasc Surg, 2002. **36**(3): p. 598-604. https://doi.org/10.1067/mva.2002.126087.

[46] Inzoli, F., et al., *Biomechanical Factors in Abdominal Aortic Aneurysm Rupture*. Eur J Vasc Surg, 1993. **7**: p. 667-667. https://doi.org/10.1016/s0950-821x(05)80714-5.

[47] Bluestein, D., et al., *Steady Flow in an Aneurysm Model: Correlation Between Fluid Dynamics and Blood Platelet Deposition*. Journal of Biomechanical Engineering, 1996. **118**(3): p. 280-286. https://doi.org/10.1115/1.2796008.

[48] Wolters, B.J.B.M., et al., *A patient-specific computational model of fluid–structure interaction in abdominal aortic aneurysms*. Med Eng Phys, 2005. **27**(10): p. 871-883. https://doi.org/10.1016/j.medengphy.2005.06.008.

[49] Vande Geest, J.P., M.S. Sacks, and D.A. Vorp, *The effects of aneurysm on the biaxial mechanical behavior of human abdominal aorta.* J Biomech, 2006. **39**(7): p. 1324-1334. https://doi.org/10.1016/j.jbiomech.2005.03.003.

[50] De Putter, S., et al., *Patient-specific initial wall stress in abdominal aortic aneurysms with a backward incremental method.* Journal of Biomechanics, 2007. **40**(5): p. 1081-1090. https://doi.org/10.1016/j.jbiomech.2006.04.019.

[51] Lederle, F.A., et al., *Prevalence and associations of abdominal aortic aneurysm detected through screening.* Annals of Internal Medicine, 1997. **126**(6): p. 441-449. https://doi.org/10.7326/0003-4819-126-6-199703150-00004.

[52] Doyle, B.J., et al., *An Experimental and Numerical Comparison of the Rupture Locations of an Abdominal Aortic Aneurysm.* Journal of Endovascular Therapy, 2009. **16**(3): p. 322-335. https://doi.org/10.1583/09-2697.1.

[53] Doyle, B.J., et al., *Experimental modelling of aortic aneurysms: novel applications of silicone rubbers.* Med Eng Phys, 2009. **31**(8): p. 1002-1012. https://doi.org/10.1016/j.medengphy.2009.06.002.

[54] Doyle, B.J., et al., *3D Reconstruction and Manufacture of Real Abdominal Aortic Aneurysms: From CT Scan to Silicone Model.* Journal of Biomechanical Engineering, 2008. **130**(3): p. 034501-5. https://doi.org/10.1115/1.2907765.

[55] Doyle , B.J., et al., *The use of silicone materials to model abdominal aortic aneurysm behaviour.*, in *SPE 1st European Conference on Medical Polymers*. 2008: Northern Ireland, Belfast.

[56] Doyle, B.J., et al., *Identification of rupture locations in patient-specific abdominal aortic aneurysms using experimental and computational techniques.* J Biomech, 2010. **43**(7): p. 1408-1416. https://doi.org/10.1016/j.jbiomech.2009.09.057.

[57] Vorp, D.A., M.L. Raghavan, and M.W. Webster, *Mechanical wall stress in abdominal aortic aneurysm: Influence of diameter and asymmetry.* Journal of Vascular Surgery, 1998. **27**(4): p. 632-639. https://doi.org/10.1016/s0741-5214(98)70227-7.

[58] Scotti, C.M., et al., *Wall stress and flow dynamics in abdominal aortic aneurysms: finite element analysis vs. fluid-structure interaction.* Comput Methods Biomech Biomed Engin, 2008. **11**(3): p. 301-322. https://doi.org/10.1080/10255840701827412.

[59] Georgakarakos, E., et al., *The role of geometric parameters in the prediction of abdominal aortic aneurysm wall stress.* Eur J Vasc Endovasc Surg, 2010. **39**(1): p. 42-48. https://doi.org/10.1016/j.ejvs.2009.09.026.

[60] Doyle , B.J., et al., *Regions of High Wall Stress Can Predict the Future Location of Rupture of Abdominal Aortic Aneurysm.* Cardiovasc Intervent Radiol, 2014. **37**(3): p. 815-818. https://doi.org/10.1007/s00270-014-0864-7.

[61] Georgakarakos, E., et al., *Peak wall stress does not necessarily predict the location of rupture in abdominal aortic aneurysms.* Eur J Vasc Endovasc Surg, 2010. **39**(3): p. 302-304. https://doi.org/10.1016/j.ejvs.2009.11.021.

[62] Helderman, F., et al., *A numerical model to predict abdominal aortic aneurysm expansion based on local wall stress and stiffness.* Med Biol Eng Comput, 2008. **46**(11): p. 1121-1127. https://doi.org/10.1007/s11517-008-0358-3.

[63] Zelaya, J.E., et al., *Improving the Efficiency of Abdominal Aortic Aneurysm Wall Stress Computations.* PLoS ONE, 2014. **9**(7): p. e101353. https://doi.org/10.1371/journal.pone.0101353.

[64] Raut, S.S., et al., *The role of geometric and biomechanical factors in abdominal aortic aneurysm rupture risk assessment.* Ann Biomed Eng, 2013. **41**(7): p. 1459-1477. https://doi.org/10.1007/s10439-013-0786-6.

[65] Vardulaki, K.A., et al., *Quantifying the risks of hypertension, age, sex and smoking in patients with abdominal aortic aneurysm.* British Journal of surgery, 2000. **87**: p. 195-200. https://doi.org/10.1046/j.1365-2168.2000.01353.x.

[66] Doyle , B.J., et al., *From Detection to Rupture: A Serial Computational Fluid Dynamics Case Study of a Rapidly Expanding, Patient-Specific, Ruptured Abdominal Aortic Aneurysm.*, in *Computational Biomechanics for Medicine*, M.K. Doyle B., Wittek A., Nielsen P., Editor. 2014, Springer: New York, NY. https://doi.org/10.1007/978-1-4939-0745-8_5.

[67] Maier, A., et al. *Impact of Model Complexity on Patient Specific Wall Stress Analyses of Abdominal Aortic Aneurysms*. in *World Congress on Medical Physics and Biomedical Engineering, September 7 - 12, 2009, Munich, Germany*. 2010. Berlin, Heidelberg: Springer Berlin Heidelberg. https://doi.org/10.1007/978-3-642-03882-2_135.

[68] Reeps, C., et al., *The impact of model assumptions on results of computational mechanics in abdominal aortic aneurysm.* J Vasc Surg, 2010. **51**(3): p. 679-688. https://doi.org/10.1016/j.jvs.2009.10.048.